

Title page

Original article

Associations among bronchioloalveolar carcinoma component, positron emission tomographic, computed tomographic findings and malignant behavior in small lung adenocarcinomas

Subhead: PET/CT and HR-CT for biology of small adenocarcinoma

*Morihito Okada, MD, PhD¹, Shunsuke Tauchi, MD¹, Koichiro Iwanaga, MD¹, Takeshi Mimura, MD¹, Yoshitaka Kitamura, MD¹, Hirokazu Watanabe, MD, PhD², Shuji Adachi, MD, PhD², Toshiko Sakuma, MD, PhD³, and Chiho Ohbayashi, MD, PhD³

Department of ¹Thoracic Surgery, ²Radiology and ³Pathology,
Hyogo Medical Center for Adults, Akashi City, Hyogo, JAPAN.

Word count: 3889 words, 2 figures, 5 tables

Key words: bronchioloalveolar carcinoma, sublobar resection, adenocarcinoma, FDG-PET/CT

*Address for reprint requests and correspondence: Morihito Okada, MD, PhD

Department of Thoracic Surgery, Hyogo Medical Center for Adults,

Kitaohji-cho13-70, Akashi City 673-8558, Hyogo, Japan

E-mail: morihito1217jp@aol.com

Telephone: 81-78-929-1151 Fax: 81-78-929-238

Abstract

Objective: The aggressiveness of small adenocarcinomas has not been fully evaluated using integrated positron emission tomography/computed tomography (PET/CT). We investigated malignant aggressiveness according to PET/CT, high-resolution computed tomography (HR-CT) findings and the proportions of pathologically defined bronchioloalveolar carcinomas (BACs) in cT1N0M0 lung adenocarcinoma.

Methods: Sixty consecutive patients with cT1N0M0 lung adenocarcinomas of 3 cm or less in diameter, underwent fluorodeoxyglucose (FDG)-PET/CT and HR-CT followed by complete tumor resection. Correlations between the proportion of BAC and maximum standardized uptake value (SUV) on PET/CT, ground-glass opacity (GGO) and tumor shadow disappearance rate (TDR) were investigated and the findings were compared with clinicopathological features.

Results: Lymphatic and vascular invasion occurred in 18 (30%) and 13 (22%) patients, respectively, whereas hilar or mediastinal lymph nodes were involved in 8 patients (13%). Maximum SUV generally seemed the most valuable predictor of lymphatic invasion, vascular invasion and nodal metastasis, compared with GGO, TDR and BAC ratios. Although the association was significant between the BAC ratio versus maximum SUV, GGO ratio and TDR (all $p < 0.0001$), maximum SUV ($R^2 = 0.245$) was less correlated with the BAC ratio than the GGO ratio ($R^2 = 0.554$) and TDR ($R^2 = 0.671$).

Conclusions: The malignant behavior of small adenocarcinomas with a lower maximum SUV and a greater proportion of GGO, TDR and BAC was less aggressive. Maximum SUV was a more powerful clinical predictor of biological tumor performance, independently of pathological BAC proportion. Preoperative assessment of maximum SUV on PET/CT in addition to the GGO ratio and TDR on HR-CT might be useful to guide treatment strategies for small adenocarcinomas.

Ultramini-Abstract

The malignant behavior of adenocarcinomas of up to 3 cm according to positron emission/computed tomography, high-resolution computed tomography and pathological examination was investigated in 60 consecutive patients who underwent surgical intervention. The maximum standardized uptake more adequately predicts the malignant aggressiveness of small adenocarcinoma than the ground-glass opacity ratio and tumor shadow disappearance rate, regardless of the proportion of bronchioloalveolar carcinoma.

Text

Introduction

Recent improvements in imaging technology and the widespread use of CT scans for screening have increased the probability of detecting small-sized lung cancers, especially adenocarcinomas, and this has led to concerns over whether some of these cancers can be sufficiently treated by sublobar resection as an alternative to lobectomy [1,2]. In fact, about 20% of clinical T1 cancers have nodal involvement and the remainder follows a more indolent biological course. Since the risk of nodal involvement and subsequent systemic metastasis is not absolutely linked to tumor size [3], the preoperative ability to distinguish biologically aggressive from indolent tumors is extremely important for an indication of sublobar resection.

On high-resolution computed tomography (HR-CT), Ground-glass opacity (GGO) defined as a misty component in lung attenuation, and tumor shadow disappearance rate (TDR) defined as the ratio of tumor area of the mediastinal window to that of the lung window, seem linked to adenocarcinoma aggressiveness and thus to the risk of nodal involvement [4,5]. In addition, bronchioloalveolar carcinomas (BACs) typified by lepidic growth along alveoli without invasive areas are indolent and basically expressed as GGO or areas of tumor shadow disappearance on HR-CT.

On the other hand, integrated positron emission tomography-computed tomography with F-18 fluorodeoxyglucose (FDG-PET/CT), is a refined type of dedicated FDG-PET that measures a standardized uptake value (SUV). This is an increasingly useful noninvasive imaging modality with which to evaluate indeterminate lung nodules, regional lymph nodes, distant metastases, tumor invasiveness and responses to chemoradiotherapy [6-14]. Furthermore, FDG-PET/CT might be able to quantify the aggressiveness of small adenocarcinomas.

Notably, preoperative imaging findings with PET/CT and HR-CT must be defined and correlated with pathological findings. Preoperatively understanding the biological features of small adenocarcinomas could provide clues to select patients for radical sublobar resection. We therefore examined correlations between SUV, GGO proportion and TDR with the BAC proportion defined on pathological sections of surgical specimens. The results of this study could improve approaches to diagnosing and treating small lung adenocarcinomas that might become a more vital part of thoracic surgical tradition.

Patients and Methods

Between October 2005 and September 2006, the same surgical team completely resected tumors and assessed ipsilateral hilar and mediastinal lymph nodes for primary cT1N0M0 lung adenocarcinomas (3 cm or less in diameter) in 60 consecutive patients. Our institutional review board approved the prospective database used in this retrospective analysis. Surgical-pathologic staging was performed according to the New International Staging System for Lung Cancer [15]. All patients underwent integrated FDG-PET/CT and HR-CT within 1 month before resection. Patients with diabetes were excluded from this study.

FDG-PET/CT scans were carried out on an integrated PET/CT scanner (Discovery ST8 PET/CT Scanner; General Electric, Milwaukee, Wis). Patients were requested to fast for 4 hours and then intravenously received 185 MBq (5 mCi) of FDG, followed by PET scanning after 40 minutes. Iterative reconstruction with CT attenuation correction was performed. Also, chest CT scan was available for visual correlation. Maximum SUV was established by drawing regions of interest on attenuation-corrected FDG-PET images around the primary tumor and calculated by the software within the PET/CT scanner using the following formula: Maximum SUV = $[C(\mu\text{Ci/mL}) / \text{ID}(\mu\text{Ci})] / w(\text{kg})$, where C is defined as activity at a pixel within the tissue identified by an regions

of interest, and ID is defined as the injected dose per kilogram of the patient's body weight (w). We adopted maximum SUV in the present analysis because it is less variable than mean SUV in measuring [16], and established a value of 2.5 g/mL or higher as positive.

Contrast-enhanced HR-CT was performed on a multi-detector CT capable of generating 16 x 0.5 mm slices (Aquilion 16SH; Toshiba Medical Systems, Tokyo, Japan). Slices with 1-mm spaces were taken through the tumor in addition to all slices with 6-mm spacing obtained from the apex of the lung to the base. The images were photographed using a window level of -600 Hounsfield units (HU) with a window width of 1700 HU (lung windows) and a level of 25 HU with a width of 350 HU (mediastinal windows). TDR and GGO were assessed by independent observers, and discrepancies in evaluation among them were resolved by averaging their determined values. The observers measured the maximum dimensions of the tumors (maxD) and the largest dimension perpendicular to the maximum axis (perD) on both the lung and mediastinal windows. As reported [4,5,17], TDR was defined as follows:

$$\text{TDR}(\%) = [1 - (\text{maxD} \times \text{perD on mediastinal windows} / \text{maxD} \times \text{perD on lung windows})] \times 100$$

The tumors resected surgically were fixed in 10% formalin and embedded in paraffin. The sections including the largest cut were stained with hematoxylin-eosin and elastica van Gieson, for histopathological examination. The estimation regarding the proportion of BAC areas relative to the whole tumors was performed by independent pathologists in the same manner as that for PET/CT and HR-CT reviews. The clinical records of all patients were also reviewed to determine age, gender, smoking status, serum carcinoembryonic antigen (CEA) level, tumor size, operative procedure, lymph node status (N factor), lymphatic invasion (Ly factor), and vascular invasion (V factor). When lymphatic and blood vessels had been invaded, adenocarcinoma cells were histopathologically identifiable in the lymphatic and blood vessel lumen, respectively. Lymphatic and blood vessels were identified based on morphology using light microscopy and elastica stain.

Peritumoral invasion (observed outside the margin of the invasive carcinoma) and intratumoral types of invasion were assessed.

The associations between clinical factors and maximum SUV, GGO ratio, TDR and BAC ratio were evaluated using the χ^2 test, or the Fisher exact tests. To elucidate variables for the prediction of nodal, lymphatic and vessel involvement, we performed logistic regression analyses. To further clarify independent variables in relation to the prediction of nodal involvement, we performed multiple logistic regression analyses using gender for category and age, CEA, maximum SUV, GGO ratio, TDR and BAC ratio as continuous variables. We also examined which of maximum SUV, GGO ratio or TDR correlated more closely with the BAC ratio using a correlation coefficient.

Results

Of 60 patients examined, 31 (52%) were women and 29 were men. The mean age was 65 years (range 34-82 years). Thirty-one patients (52%) were smokers, of whom 17 currently smoked, and 29 had never smoked. Forty-eight patients (80%) had a normal preoperative CEA level, the upper limit of which was 5.0 ng/mL. Half of the patients had a primary tumor with a diameter of 20 mm or less and the other half had a tumor of 21 to 30 mm in diameter. Lobectomy was the most frequently applied type of resection (n=44, 73%) and 16 patients underwent segmental resections. The reasons for sublobar resection included radical segmentectomy for tumors 2 cm or smaller in 11 patients and compromised reserve in 5. Pneumonectomy was never performed and wedge resection was excluded because nodal status could not be histopathologically confirmed. All patients had curative R0 resections. Lymphatic and vascular invasion occurred in 18 (30%) and 13 (22%) patients, respectively. Fifty-two patients (87%) had no nodal involvement, whereas hilar or mediastinal lymph node involvement was found in 8 patients (13%).

The clinical features of the patients in relationship to maximum SUV on PET/CT are summarized in Table 1. Larger tumors ($p=0.0061$) and a high preoperative CEA value ($p=0.0169$) were more frequent in patients with a positive maximum SUV. Maximum SUV did not differ with age, gender, smoking status and operative procedure. The CEA value was frequently high in patients whose proportions of GGO and TDR on HR-CT and pathological BAC on surgical specimen (Table 2,3 and 4) were below 50% proportion ($p=0.0446$, $p=0.0498$ and $p=0.0253$, respectively).

We then analyzed the predictors for lymphatic invasion, vascular invasion and nodal metastasis (Table 5). Maximum SUV, GGO proportion, TDR and BAC proportion were all found to be significant predictors of lymphatic ($p<0.0001$, $p=0.0189$, $p=0.0020$ and $p=0.0005$, respectively) and vascular ($p<0.0001$, $p=0.0433$, $p=0.0256$ and $p<0.0001$, respectively) invasion. Whereas maximum SUV, TDR and BAC proportion were significant predictors of nodal metastasis ($p=0.0019$, $p=0.0201$ and $p=0.0053$, respectively), the GGO proportion was not significantly useful for predicting nodal status ($p=0.2487$). Overall, maximum SUV, BAC ratio, TDR, and the GGO ratio in that order can likely reflect tumor aggressiveness. A multivariate analysis to determine independent predictors of pathologic nodal status (Table 6) revealed that none of age, gender and CEA were significant in any model. Maximum SUV ($p=0.0199$), TDR ($p=0.0136$) and BAC ratio ($p=0.0375$) were significantly useful predictors of nodal status although GGO ratio and nodal status correlated marginally but not significantly ($p=0.0800$).

Last, we performed logistic regression analyses to clarify which radiographic parameter of maximum SUV, GGO ratio or TDR correlated better with a pathologic BAC ratio (Figure 1). Although a significant correlation was found between BAC ratio versus maximum SUV, GGO ratio and TDR (all $p<0.0001$), maximum SUV ($R^2 = 0.245$) had a poorer association with BAC ratio compared with GGO ratio ($R^2 = 0.554$) and TDR ($R^2 = 0.671$). These data demonstrated that both TDR and GGO ratio on HR-CT were well correlated with pathologic BAC ratio and that

maximum SUV on PET/CT had a much less impact as a preoperative indicator of pathologic BAC proportion.

Discussion

Although the proportion of the BAC component can mirror the malignant grade of small adenocarcinoma [4,18,19], it is defined on post-surgical specimens. Since the parts indicating GGO or TDR on HR-CT seemed to closely correlate with BAC area, the proportion of GGO and TDR might be linked to tumor aggressiveness and subsequently to risk for nodal metastases and survival [4,5,17]. Characterizing and quantifying these findings on HR-CT, especially GGO, have been relatively subjective, since inter-observer discrepancies might have affected visual estimations.

Cerfolio and colleagues have reported that maximum SUV of a non-small cell lung cancer nodule on dedicated PET is an independent predictor of tumor characteristics for stage, recurrence and survival [11]. However, the utility of FDG-PET/CT in predicting the biological features of small adenocarcinomas, especially BACs remains obscure. While approximately 85% of non-small cell lung cancers are FDG positive, roughly 50% of adenocarcinomas with a BAC component are FDG positive and pure BAC is more likely to escape detection with FDG-PET [20,21]. Lower metabolic activity in adenocarcinomas containing a BAC component is assumed to be secondary to the slower pace of BAC proliferation compared with other adenocarcinomas. If higher metabolic activity is linked to more tumor aggressiveness, FDG avidity (maximum SUV) might identify a group of adenocarcinomas that is more likely to have high-grade malignant behavior.

In the present series, adenocarcinoma with a high maximum SUV as well as a low percentage of GGO, TDR or BAC was more frequently associated with an increase in the serum CEA level. Pre-surgical serum CEA values are important in identifying patients at high risk of potential

advanced disease and poor survival, and whose specificity is higher for adenocarcinoma than squamous cell carcinoma [22,23]. The present study also uncovered an even closer relationship between maximum SUV and lymphatic, blood vessel and lymph node involvement compared with GGO, TDR and BAC. Surprisingly, maximum SUV obtained preoperatively could be a more reliable indicator for predicting tumor malignancy than BAC proportion obtained postoperatively. These results suggested that maximum SUV is a reasonable surrogate marker of adenocarcinoma invasiveness and that FDG-PET/CT could be a powerful prognostic tool with which to identify patients at high and low risk of recurrence after complete resection of small adenocarcinomas with or without a BAC component.

The relationships between the pathological BAC ratio and radiographic maximum SUV, GGO ratio and TDR in small adenocarcinomas are of interest in helping to understand the fundamental role of maximum SUV. The extent of both the GGO area and TDR closely correlated with that of BAC growth. We however emphasize that maximum SUV, in comparison with the GGO ratio and TDR, was less associated with the BAC proportion. This discrepancy can be essential when considering the underlying significance of maximum SUV. That is, graphic maximum SUV unlike the GGO ratio or TDR is less able to reflect the pathological BAC proportion, and might be an imperative predictor for the grade of tumor malignancy independently of the BAC component.

The current relative decrease in the size of resected lung tumors allows a choice of various surgical options [2]. Choosing radical sublobar resection for patients that could tolerate lobectomy requires better methods of preoperatively distinguishing early indolent, from advanced aggressive cancers. However, no absolutely accurate preoperative indicators of tumor behavior have been defined although several studies have reported that the GGO ratio and TDR on HR-CT as well as tumor size and histology are useful [3-5,17]. Our series showed that maximum SUV on PET/CT is a potentially promising parameter for determining an indication for radical sublobar resection. We also examined the relationship between maximum SUV and tumor size in

cT1N0M0 adenocarcinomas (Fig. 2). We found that the larger the tumor, the higher was the maximum SUV, and both of these factors can predict tumor invasiveness and nodal metastases. Thus, FDG-PET/CT in addition to HR-CT might be significantly useful for an indication of radical sublobar resection and a reduction in nodal dissection for surgically treating small adenocarcinomas, which requires further confirmation in a large cohort.

References

1. Ginsberg RJ, Rubinstein LV. Randomized trial of lobectomy versus limited resection for T1 N0 non-small cell lung cancer. Lung Cancer Study Group. *Ann Thorac Surg.* 1995;60:615–22.
2. Okada M, Koike T, Higashiyama M, Yamato Y, Kodama K, Tsubota N. Radical sublobar resection for small-sized non-small cell lung cancer: a multicenter study. *J Thorac Cardiovasc Surg.* 2006;132:769-75.
3. Okada M, Nishio W, Sakamoto T, Uchino K, Yuki T, Nakagawa M, et al. Effect of tumor size on prognosis in patients with non-small cell lung cancer: the role of segmentectomy as a type of lesser resection. *J Thorac Cardiovasc Surg.* 2005;129: 87-93.
4. Okada M, Nishio W, Sakamoto T, Uchino K, Hanioka K, Ohbayashi C, et al. Correlation between computed tomographic findings, bronchioloalveolar carcinoma component, and biologic behavior of small-sized lung adenocarcinomas. *J Thorac Cardiovasc Surg.* 2004;127: 857-61.
5. Okada M, Nishio W, Sakamoto T, Uchino K, Tsubota N. Discrepancy of computed tomographic image between lung and mediastinal windows as a prognostic implication in small lung adenocarcinoma. *Ann Thorac Surg.* 2003;76:1828-32.
6. Nomori H, Watanage K, Ohtsuka T, Naruke T, Suemasu K, Kobayashi T, et al. Fluorine 18-tagged fluorodeoxyglucose positron emission tomographic scanning to predict lymph node metastasis, invasiveness, or both, in clinical T1 N0 M0 lung adenocarcinoma. *J Thorac Cardiovasc Surg.* 2004;128: 396-401.
7. Cerfolio RJ, Ojha B, Bryant AS, Bass CS, Bartalucci AA, Mountz JM. The role of FGD-PET scan in staging patients with non small cell carcinoma. *Ann Thorac Surg.* 2003;76:861–6.

8. Cerfolio RJ, Bryant AS, Ojha B. Restaging patients with N2 (stage IIIa) non-small cell lung cancer after neoadjuvant chemoradiotherapy: a prospective study. *J Thorac Cardiovasc Surg.* 2006;131:1229-35.
9. McCain TW, Dunagan DP, Chin R Jr, Oaks T, Harkness BA, Haponik EF. The usefulness of positron emission tomography in evaluating patients for pulmonary malignancies, *Chest.* 2000;118:1610–1615.
10. Pieterman RM, van Putten JW, Meuzelaar JJ, Mooyaart EL, Vaalburg W, Koeter GH, et al. Preoperative staging of non-small cell lung cancer with positron emission tomography. *N Engl J Med.* 2000;343:254–61.
11. Cerfolio RJ, Bryant AS, Ohja B, Bartolucci AA. The maximum standardized uptake values on positron emission tomography of a non-small cell lung cancer predict stage, recurrence, and survival. *J Thorac Cardiovasc Surg.* 2005;130: 151-159.
12. Dhital K, Saunders CAB, Seed PT, O'Doherty MJ, Dussek J. [¹⁸F]Fluorodeoxyglucose positron emission tomography and its prognostic value in lung cancer. *Eur J Cardiothorac Surg.* 2000;18: 425-428.
13. Vansteenkiste J, Fischer BM, Doms C, Mortensen J. Positron-emission tomography in prognostic and therapeutic assessment of lung cancer: systematic review. *The Lancet Oncology.* 2004;5: 531-540.
14. Ahuja V, Coleman RE, Herndon J, Patz EF Jr. The prognostic significance of fluorodeoxyglucose positron emission tomography imaging for patients with nonsmall cell lung carcinoma. *Cancer.* 1998;83:918-924.
15. Mountain CF. Revisions in the International System for Staging Lung Cancer. *Chest.* 1997;111:1710–17.
16. Lee JR, Madsen MT, Bushnell D, Menda Y. A threshold method to improve standardized uptake value reproducibility. *Nucl Med Commun.* 2000;21:685–90.

17. Takamochi K, Nagai K, Yoshida J, Suzuki K, Ohde Y, Nishimura M, et al. Pathologic NO status in pulmonary adenocarcinoma is predictable by combining serum carcinoembryonic antigen level and computed tomographic findings. *J Thorac Cardiovasc Surg.* 2001;122:325–30.
18. Noguchi M., Morikawa A, Kawasaki M, Matsuno Y, Yamada T, Hirohashi S, et al. Small adenocarcinoma of the lung. Histologic characteristics and prognosis. *Cancer.* 1995;75:2844–52.
19. Goldstein NS, Mani A, Chmielewski G, Welsh R, Pursel S. Prognostic factors in T1 NO MO adenocarcinomas and bronchioloalveolar carcinomas of the lung. *Am J Clin Pathol.* 1999;112 :391–402.
20. Yap CS, Schiepers C, Fishbein MC, Phelps ME, Czernin J. FDG-PET imaging in lung cancer: how sensitive is it for bronchioloalveolar carcinoma? *Eur J Nucl Med Mol Imaging.* 2002;29:1166-73.
21. Heyneman LE, Patz EF. PET imaging in patients with bronchioloalveolar cell carcinoma. *Lung cancer.* 2002;38:261-6.
22. Okada M, Nishio W, Sakamoto T, Uchino K, Yuki T, Nakagawa A, et al. Prognostic significance of perioperative serum carcinoembryonic antigen in non-small cell lung cancer: analysis of 1,000 consecutive resections for clinical stage I disease. *Ann Thorac Surg.* 2004;78:216-21.
23. Okada M, Nishio W, Sakamoto T, Uchino K, Yuki T, Nakagawa A, et al. Effect of histologic type and smoking status on interpretation of serum carcinoembryonic antigen value in non-small cell lung carcinoma. *Ann Thorac Surg.* 2004;78:1004-9.

Table 1. Clinical characteristics of patients with cT1N0M0 adenocarcinoma relative to the level of maximum SUV on FDG-PET/CT images

		Maximum SUV \leq 2.5	Maximum SUV $>$ 2.5	P value
		N=39	N=21	
Age(y)(means \pm SD)		64.3 \pm 9.8	66.1 \pm 9.2	0.4939
Gender	Male	17	12	0.4184
	Female	22	9	
Smoking status	Smoker	18	13	0.2874
	Nonsmoker	21	8	
CEA(ng/ml)	\leq 5	35	13	0.0169
	$>$ 5	4	8	
Tumor size(mm)	T \leq 20	25	5	0.0061
	20<T \leq 30	14	16	
Procedure	Lobectomy	27	17	0.3767
	Segmentectomy	12	4	

SUV, standardized uptake value; FDG-PET/CT, positron emission tomography-computed tomography with F-18 fluorodeoxyglucose; SD, standard deviation; CEA, carcinoembryonic antigen.

Table 2. Clinical characteristics of patients with cT1N0M0 adenocarcinoma relative to the proportion of GGO on HR-CT images

		GGO \geq 50%	GGO<50%	P value
		N=20	N=40	
Age(y)(means \pm SD)		65.4 \pm 8.9	64.1 \pm 10.9	0.6367
Gender	Male	7	22	0.1772
	Female	13	18	
Smoking status	Smoker	8	23	0.2749
	Nonsmoker	12	17	
CEA(ng/ml)	\leq 5	19	29	0.0466
	>5	1	11	
Tumor size(mm)	T \leq 20	13	17	0.1702
	20<T \leq 30	7	23	
Procedure	Lobectomy	14	30	0.7604
	Segmentectomy	6	10	

GGO, ground-glass opacity; HR-CT, high-resolution computed tomography; SD, standard deviation; CEA, carcinoembryonic antigen.

Table 3. Clinical characteristics of patients with cT1N0M0 adenocarcinoma relative to TDR on HR-CT images

		TDR \geq 50%	TDR<50%	P value
		N=32	N=28	
Age(y)(means \pm SD)		66.1 \pm 9.5	63.9 \pm 9.6	0.3632
Gender	Male	13	16	0.3005
	Female	19	12	
Smoking status	Smoker	16	15	0.8017
	Nonsmoker	16	13	
CEA(ng/ml)	\leq 5	29	19	0.0498
	>5	3	9	
Tumor size(mm)	T \leq 20	20	10	0.0692
	20<T \leq 30	12	18	
Procedure	Lobectomy	21	23	0.2417
	Segmentectomy	11	5	

TDR, tumor shadow disappearance rate; HR-CT, high-resolution computed tomography; SD, standard deviation; CEA, carcinoembryonic antigen.

Table 4. Clinical characteristics of patients with cT1N0M0 adenocarcinoma relative to the proportion of BAC on pathological examination

		BAC \geq 50%	BAC<50%	P value
		N=28	N=32	
Age(y)(means \pm SD)		65.4 \pm 10.9	64.5 \pm 8.4	0.7305
Gender	Male	10	19	0.0773
	Female	18	13	
Smoking status	Smoker	12	19	0.3005
	Nonsmoker	16	13	
CEA(ng/ml)	\leq 5	26	22	0.0253
	>5	2	10	
Tumor size(mm)	T \leq 20	18	12	0.0692
	20<T \leq 30	10	20	
Procedure	Lobectomy	20	24	0.7780
	Segmentectomy	8	8	

BAC, bronchioloalveolar carcinoma; SD, standard deviation; CEA, carcinoembryonic antigen.

Table 5. Univariate analysis of predictors for Ly (lymphatic invasion) factor, V (vascular invasion) factor and N (nodal metastasis) status

Factors	Favorable	Unfavorable	Odds ratio (95%CI)	P value
For Ly factor				
Maximum SUV	≤2.5	>2.5	17.50 (4.420-69.283)	<0.0001
GGO ratio	≥50	<50	6.00 (1.221-9.481)	0.0189
TDR	≥50	<50	7.00 (1.940-25.255)	0.0020
Pathologic BAC ratio	≥50	<50	13.00 (2.634-64.163)	0.0005
.....				
For V factor				
Maximum SUV	≤2.5	>2.5	(-)	<0.0001
GGO ratio	≥50	<50	8.142 (0.9759-67.947)	0.0433
TDR	≥50	<50	5.37 (1.301-22.172)	0.0256
Pathologic BAC ratio	≥50	<50	(-)	<0.0001
.....				
For N factor				
Maximum SUV	≤2.5	>2.5	19.00(2.141-168.660)	0.0019
GGO ratio	≥50	<50	4.03 (0.460-35.299)	0.2487
TDR	≥50	<50	10.33 (1.183-90.260)	0.0201
Pathologic BAC ratio	≥50	<50	(-)	0.0053

CI, confidence interval; SUV, standardized uptake value; GGO, ground-glass opacity; TDR, tumor shadow disappearance rate; BAC, bronchioloalveolar carcinoma.

Table 6. Logistic regression analysis of clinicopathological factors for positive predictive values of pathologic nodal status.

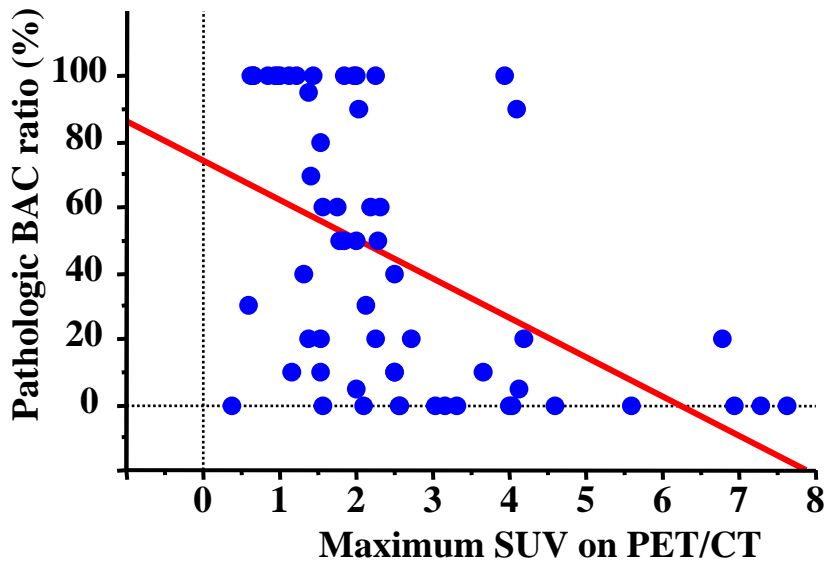
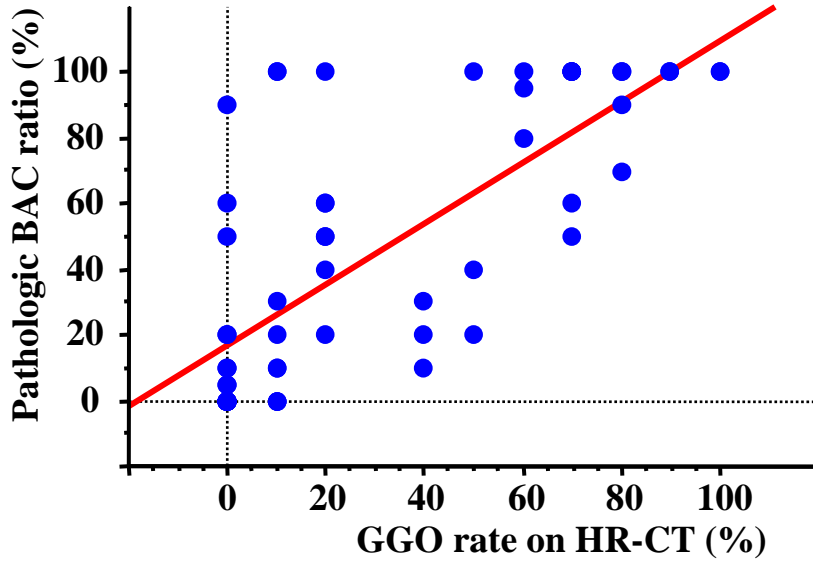
Factors	Odds ratio (95%CI)	P value
Model 1 (R ² =0.146)		
Age	0.960 (0.880-1.048)	0.3613
Gender	0.530 (0.086-3.279)	0.4948
CEA	0.999 (0.774-1.290)	0.9936
Maximum SUV	1.709 (1.088-2.684)	0.0199
.....		
Model 2 (R ² =0.136)		
Age	0.949 (0.866-1.039)	0.2577
Gender	0.811 (0.164-4.021)	0.7977
CEA	1.026 (0.813-1.295)	0.8270
GGO ratio	0.961 (0.920-1.005)	0.0800
.....		
Model 3 (R ² =0.282)		
Age	0.948 (0.858-1.047)	0.2925
Gender	0.858 (0.143-5.153)	0.8669
CEA	1.013 (0.751-1.367)	0.9334
TDR	0.937 (0.890-0.987)	0.0136
.....		
Model 4 (R ² =0.208)		
Age	0.960 (0.869-1.061)	0.4247
Gender	0.589 (0.113-3.070)	0.5295
CEA	0.989 (0.776-1.261)	0.9312
Pathologic BAC ratio	0.958 (0.920-0.998)	0.0375

CI, confidence interval; CEA, carcinoembryonic antigen; SUV, standardized uptake value; GGO, ground-glass opacity; TDR, tumor shadow disappearance rate; BAC, bronchioloalveolar carcinoma. Category for gender and continuous variables for age, CEA, maximum SUV, GGO ratio, TDR and BAC ratio.

Legends for figures

Fig. 1. Regression parameters of radiographic findings and pathological results in cT1N0M0 adenocarcinomas. A, Correlation between maximum SUV on FDG-PET/CT and pathological BAC ratio ($R^2=0.245$, $p<0.0001$). B, Correlation between GGO ratio on HR-CT and pathological BAC ratio ($R^2=0.554$, $p<0.0001$). C, Correlation between TDR on HR-CT and pathological BAC ratio ($R^2=0.671$, $p<0.0001$).

Fig. 2. Relationship between tumor size and maximum SUV level in cT1N0M0 adenocarcinomas. Squares, nodal metastasis; triangles, no nodal metastasis but lymphatic or vascular invasion; circles, no findings of nodal metastasis, lymphatic and vascular invasion.

A**B****C**